LIMNOLOGY
and
OCEANOGRAPHY: METHODS

Limnol. Oceanogr.: Methods 8, 2010, 610–627

Evaluating oxygen fluxes using microprofiles from both sides of the sediment–water interface

Lee D. Bryant,[1,5] Daniel F. McGinnis,[2] Claudia Lorrai,[3,4] Andreas Brand,[3,6] John C. Little,[1] Alfred Wüest[3,4]*

[1]Civil and Environmental Engineering, Virginia Tech, Blacksburg, Virginia, USA
[2]IFM-GEOMAR, Leibniz Institute of Marine Sciences, RD2 Marine Biogeochemistry, Kiel, Germany
[3]Eawag (Swiss Federal Institute of Aquatic Science and Technology), Surface Waters – Research and Management, Kastanienbaum, Switzerland
[4]Institute of Biogeochemistry and Pollutant Dynamics, ETH Zurich, Switzerland
[5]Current address: Civil and Environmental Engineering, Duke University, Durham, North Carolina, USA
[6]Current address: Civil and Environmental Engineering, University of California, Berkeley, California, USA

Abstract

Sediment–water fluxes are influenced by both hydrodynamics and sediment biogeochemical processes. However, fluxes at the sediment–water interface (SWI) are almost always analyzed from either a water- or sediment-side perspective. This study expands on previous work by comparing water-side (hydrodynamics and resulting diffusive boundary layer thickness, δ_{DBL}) and sediment-side (oxygen consumption and resulting sediment oxic zone) approaches for evaluating diffusive sediment oxygen uptake rate (J_{O2}) and δ_{DBL} from microprofiles. Dissolved oxygen microprofile and current velocity data were analyzed using five common methods to estimate J_{O2} and δ_{DBL} and to assess the robustness of the approaches. Comparable values for J_{O2} and δ_{DBL} were obtained (agreement within 20%), and turbulence-induced variations in these parameters were uniformly characterized with the five methods. J_{O2} estimates based on water-side data were consistently higher (+1.8 mmol m^{-2} d^{-1} or 25% on average) and δ_{DBL} estimates correspondingly lower (–0.4 mm or 35% on average) than those obtained using sediment-side data. This deviation may be attributed to definition of the sediment–water interface location, artifacts of the methods themselves, assumptions made on sediment properties, and/or variability in sediment oxygen-uptake processes. Our work emphasizes that sediment-side microprofile data may more accurately describe oxygen uptake at a particular location, whereas water-side data are representative of oxygen uptake over a broader sediment area. Regardless, our overall results show clearly that estimates of J_{O2} and δ_{DBL} are not strongly dependent on the method chosen for analysis.

Problems related to low levels of dissolved oxygen (O_2) in aquatic ecosystems are growing on a global scale (Jankowski et al. 2006; Zimmerman et al. 2008). O_2 depletion in stratified waters is largely controlled by sediment O_2 uptake, particularly in organic-rich environments (Higashino et al. 2004). Flux of O_2 across the sediment–water interface (SWI) may be governed by near-sediment hydrodynamic processes or by O_2 consumption within the sediment (Gundersen and Jørgensen 1990; Jørgensen and Boudreau 2001; Glud et al. 2007). Turbulence in the bottom boundary layer (BBL) controls the thickness (δ_{DBL}) of the diffusive boundary layer (DBL), the millimeter-scale region immediately above the sediment that typically regulates mass transport of O_2 to the SWI in non-advective, water-side–controlled systems (Jørgensen and Revsbech 1985; Lorke et al. 2003; Bryant et al. 2010). Within the sediment, the distribution of O_2 is then determined by a balance between the amount of O_2 supplied via diffusion and/or other transport processes (e.g., bioturbation) and the amount of O_2 used by biogeochemical oxidation processes (Berg et al. 2003). Quantifying the O_2 flux into the sediment, or the sediment O_2 uptake

*Corresponding author: E-mail: lebryan1@vt.edu

Acknowledgments

We are grateful to Peter Berg, Miki Hondzo, Ronnie Glud, Lars Damgaard, and Beat Müller for discussion and advice. We also thank Lorenzo Rovelli, Michi Schurter, Christian Dinkel, and Mathias Kirf, who provided invaluable assistance in the field and with equipment, and Doris Hohmann for polychaete assessment. We appreciate the constructive criticism of Clare Reimers and two anonymous reviewers. Gay Bryant kindly improved grammar and figures. This research has been funded in part by the U.S. Environmental Protection Agency (EPA) under the Science to Achieve Results (STAR) Graduate Fellowship Program. EPA has not officially endorsed this publication and the views expressed herein may not reflect the views of the EPA. This research was also supported by the U.S. National Science Foundation (NSF) through the Integrative Graduate Education and Research Traineeship (IGERT) program (DGE 0504196) and the Swiss National Science Foundation, grants 200020-111763 and 200020-120128.

DOI 10:4319/lom.2010.8.610

rate (J_{O2}), is fundamental in characterizing the availability of O_2 and corresponding ecological conditions in an aquatic system.

A wealth of literature exists on the various methods used for estimating J_{O2} (Jørgensen and Revsbech 1985; Nishihara and Ackerman 2007; Glud 2008). J_{O2} is typically evaluated from either a water- or a sediment-side perspective (O'Connor et al. 2009). Considerable research has focused on hydrodynamic controls of δ_{DBL} and corresponding O_2 transport to the sediment (Boudreau 2001; Lorke et al. 2003; Hondzo et al. 2005). Water-side, δ_{DBL}-based approaches are simpler because they do not account for O_2 consumption within the sediment and thus only diffusive mass transfer is considered (Glud 2008; O'Connor and Harvey 2008). However, both rapid turbulence-driven variations in δ_{DBL} and the short residence time of O_2 in the DBL cause δ_{DBL} to be a difficult parameter to resolve (Røy et al. 2004; O'Connor and Hondzo 2008). Furthermore, microsensor measurements of the DBL can disrupt boundary-layer flow, leading to compression of the DBL and thus changing δ_{DBL} (Glud et al. 1994).

Whereas problems with characterizing a transient δ_{DBL} are avoided by using sediment-side methods, there are additional complexities related to O_2 transport and consumption processes within the sediment (Glud 2008). Sediment-side data are often more difficult to interpret due to natural sediment heterogeneity (e.g., small-scale variations in porosity and grain size; Maerki et al. 2004). Variations in sediment O_2 levels are more site-specific owing to sediment heterogeneity, while relatively uniform water-side O_2 concentrations are maintained by lateral advection and mixing in the BBL, which provide an averaging effect on localized influences (O'Connor and Hondzo 2008). Sediment O_2 consumption processes can vary spatially (e.g., increased reactive surface area due to microtopography; Røy et al. 2002) and/or occur nonlocally (e.g., small-scale variation in benthic communities; Rabouille et al. 2003; Glud et al. 2009). Despite complications associated with localized sediment heterogeneity, porewater O_2 profile data can reveal important information about the sediment O_2 consumption rate (R_{O2}), the extent of the sediment oxic zone (Epping and Helder 1997; Berg et al. 1998; Bryant et al. 2010), and solute dynamics (Berg et al. 2007a; Glud et al. 2007; Brand et al. 2009).

Although numerous approaches are used for assessing J_{O2}, no single method has been shown to be optimal, and further evaluation of how the various methods compare is needed (Nishihara and Ackerman 2007; Glud 2008). Furthermore, because sediment O_2 uptake can be affected by processes on both sides of the SWI, evaluating J_{O2} from a one-sided perspective could result in different and biased interpretations of J_{O2} and R_{O2}. Using in situ velocity and O_2 microprofile data obtained during a companion study on the dynamic nature of J_{O2} (Bryant et al. 2010), the present work evaluates the robustness of several established methods for diffusive flux estimation based on both water- and sediment-side microprofiles. Some of the methods assessed have thus far been applied primarily in laboratory-based studies and/or rarely in situ (O'Connor and Hondzo 2008; Brand et al. 2009). The advantages and limitations of the different methods are discussed with respect to analytical approach and applicability. To our knowledge, while estimations of J_{O2} based on (1) bottom boundary currents, (2) the vertical distribution of O_2 above the sediment, and (3) sediment porewater concentration data have been well justified in previous work (Jørgensen and Revsbech 1985; Rasmussen and Jørgensen 1992; Lorke et al. 2003), this is one of the first studies that incorporates all three of these components into a comprehensive evaluation of J_{O2} and δ_{DBL} using in situ data.

Materials and procedures

Study site and in situ instrumentation—During a 12-h field campaign in Lake Alpnach, Switzerland, on August 27–28, 2007, high-resolution SWI microprofile and velocity data were collected at a depth of 22 m to determine J_{O2} and δ_{DBL}. Basic information on the experimental setup used is described here, with additional details included in the companion paper (Bryant et al. 2010). Frequently used acronyms and notations are defined in Table 1.

High-resolution O_2 profiles were measured across the SWI using a microprofiler (MP4; Unisense A/S) equipped with a Clark-type O_2 microsensor (100-µm outer tip diameter and spatial resolution, membrane diameter 3–10 µm, negligible stirring sensitivity, and 90% response time in <8 s). Profiles were measured continuously (profile duration of ~50 min) at the following resolution: 10-mm increments from 10 cm to 1 cm above the SWI, 1-mm increments from 1 cm to 0.5 cm above the SWI, and 0.1-mm increments from 0.5 cm above to 0.5 cm below the SWI. Profiles were obtained at the smallest vertical resolution possible (100 µm, as defined by sensor-tip diameter) near the SWI to maximize the number of data points characterizing changes in the O_2 concentration gradient in this region. Microsensors of 100-µm diameter were used to balance spatial resolution and robustness. After a pause between measurements to establish equilibrium, 10 data points were collected at a rate of 1 Hz at each depth; no trend in variation of the data set was evident, confirming that data aliasing did not occur. Fourteen O_2 profiles were obtained during our 12-h campaign, and the O_2 profile number (1–14) is used for comparison of results. Although the profiles were obtained at the same location, artifacts from repeated profiling are assumed to be negligible based on (1) the absence of consistent changes (e.g., oxic regions) after reprofiling (supported by work by B. Müller [unpubl.] and Lorke et al. 2003); (2) the high sediment porosity (≥0.95; discussed below); and (3) the short residence time of the upper sediment (<10 min; Bryant et al. 2010). An O_2 logger (TDO-2050; RBR Ltd.) was mounted on the microprofiler 8 cm above the sediment for independent measurements of BBL O_2 concentrations. These TDO data, collected at 1 Hz, were used with O_2 microsensor measurements taken in the anoxic sediment to calibrate the O_2 microsensor. The TDO-2050 has a 90% response time of

Table 1. Frequently used acronyms and notations.

ADV	acoustic Doppler velocimeter; used to obtain velocity data for ε and u_* estimations at 10 cm above SWI
BBL	bottom boundary layer
D	molecular diffusion coefficient of O_2 in water ($m^2\ d^{-1}$)
D_s	molecular diffusion coefficient of O_2 in sediment corrected for tortuosity where $D_s = \varphi D$ ($m^2\ d^{-1}$)
D_b	biodiffusion coefficient for O_2 ($m^2\ d^{-1}$)
DBL	diffusive boundary layer
C_{bulk}	concentration of O_2 in bulk BBL (μmol L^{-1})
C_{SWI}	concentration of O_2 at SWI (μmol L^{-1})
h	height above SWI (mm)
J_{O2}	diffusive sediment O_2 uptake rate at SWI (mmol $m^{-2}\ d^{-1}$)
Methods	
curvefit	analytical method based on best fit of polynomial defining sediment porewater profile
direct	analytical method based on directly measuring δ_{DBL} from linear DBL region of microprofile
model	analytical method based on predicting δ_{DBL} required to model sediment porewater profile via AQUASIM
u_*	analytical method based on estimating δ_{DBL} as a function of friction velocity
zonefit	analytical method based on defining multiple zero-order consumption zones to characterize sediment porewater profile via PROFILE
O_2	dissolved oxygen (μmol L^{-1})
R_{O2}	O_2 consumption rate in sediment, defined volumetrically (R_{O2v}) or areally (R_{O2a})
R_{O2a}	areal O_2 consumption rate in sediment (mmol $m^{-2}\ d^{-1}$) where $R_{O2a} = \int R_{O2v} dz$
R_{O2v}	volumetric O_2 consumption rate in sediment (mmol $m^{-3}\ d^{-1}$)
SWI	sediment–water interface
u_*	friction velocity (cm s^{-1})
z	depth below SWI (mm)
z_{max}	depth of sediment oxic zone (mm)
δ_{DBL}	diffusive boundary layer thickness (mm)
ε	dissipation rate of turbulent kinetic energy (W kg^{-1})
φ	porosity (void volume per total sediment volume; dimensionless)
σ	standard deviation (units correspond to parameter of interest)
$\partial C/\partial t$	temporal change in O_2 concentration (mmol $m^{-3}\ d^{-1}$)
$(\partial C/\partial z)_s$	O_2 concentration gradient in sediment at the SWI (mmol m^{-4})
$(\partial C/\partial z)_w$	O_2 concentration gradient in DBL water (mmol m^{-4})

<10 s, measurement range 0% to 150% O_2 saturation, resolution ±1% O_2 saturation, and accuracy ±2% O_2 saturation. TDO-2050 data were calibrated via Winkler titration of water samples obtained from the same depth with a Niskin bottle.

Water-velocity time series corresponding to each O_2 profile were collected continuously at a single point using an acoustic Doppler velocimeter (ADV; Vector, Nortek). The ADV, fixed vertically on a tripod with the sampling volume positioned 15 cm below the ADV transducer and 10 cm above the sediment, continuously measured three-dimensional velocity data at 32 Hz with an accuracy of 0.5% of the measured value or ±0.1 cm s^{-1}. ADV velocity data were used to analyze the current structure and to characterize turbulence and friction velocity within the law-of-the-wall layer.

Turbulence analyses—Turbulence in the BBL was defined by the rate of dissipation of turbulent kinetic energy ε (W kg^{-1}) using the inertial dissipation method (Grant et al. 1962). Additional details on how turbulence was analyzed may be found in Bryant et al. (2010). Average ε values were assessed based on the duration of each O_2 profile, and hence ε estimates represent a time span of ~50 min. Because turbulence is highly intermittent, dissipation is averaged by assuming log-normal distribution. Standard deviations of ln(ε), or the intermittency of ε, were evaluated using the method of Baker and Gibson (1987).

Friction velocity analyses—Friction velocity (u_*) quantifies the stress of BBL currents on the sediment. Law-of-the-wall theory and estimated mean ε values were used to calculate u_* at a height (h) of 10 cm above the sediment (Lorke et al. 2003):

$$u_* = \sqrt[3]{\varepsilon \kappa h} \quad [\text{m s}^{-1}] \tag{1}$$

where κ (von Karman constant) is 0.41.

Methods for J_{O2} analyses—Five different methods (direct, u_*, curvefit, zonefit, and model; Table 1) were used to analyze J_{O2} and δ_{DBL} using data collected on both sides of the SWI (Fig. 1). Water-side O_2 microprofile data were used for the direct method and the u_* method, which also incorporates ADV velocity data. Sediment-side O_2 microprofile data were analyzed with polynomial equations (curvefit method) and using

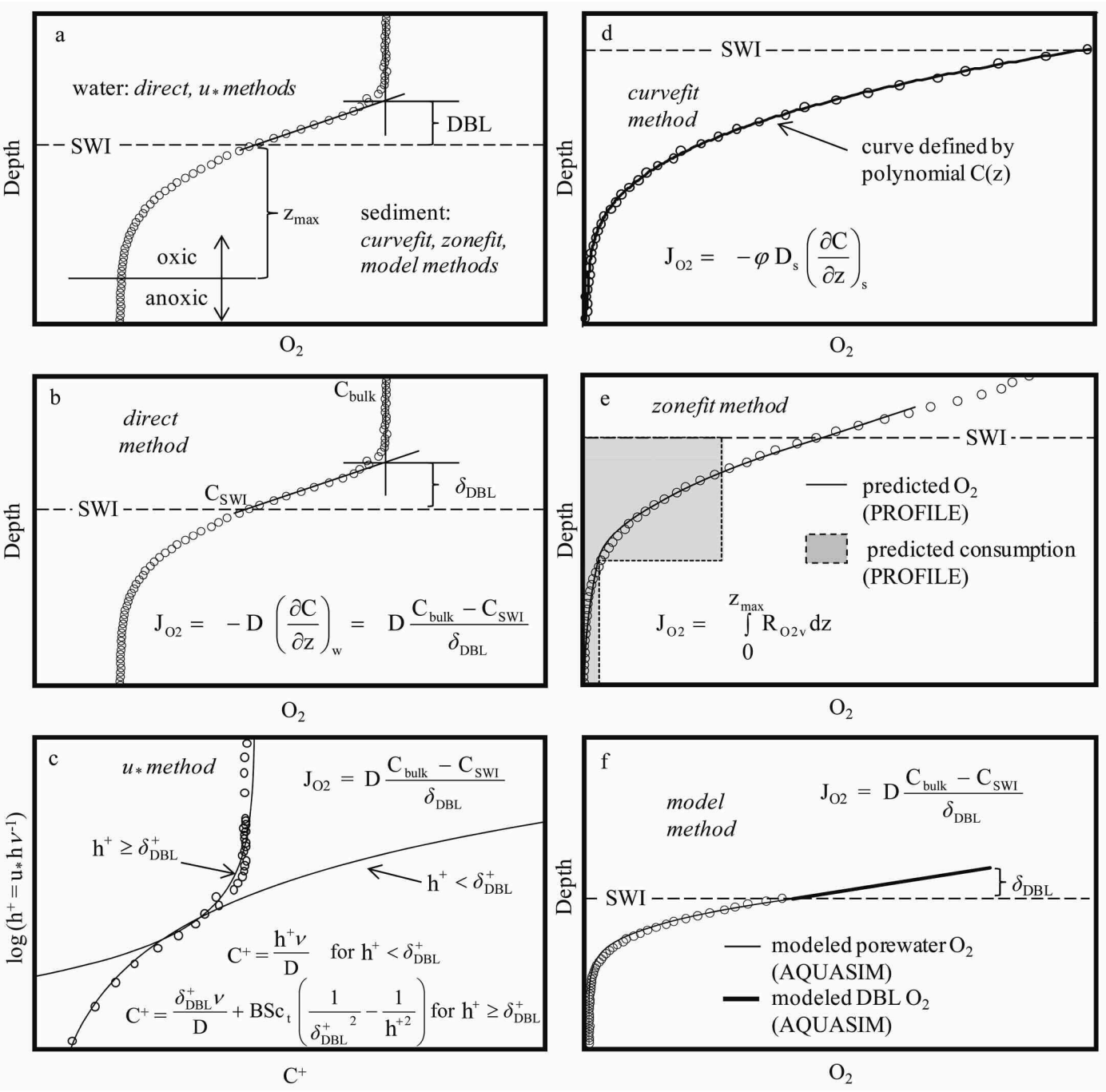

Fig. 1. Components of a dissolved oxygen (O_2) profile and the five methods used to estimate sediment O_2 uptake rate (J_{O2}) and diffusive boundary layer thickness (δ_{DBL}) are detailed using a sample O_2 profile (profile 14, obtained at 08:16 h on August 28, 2007). Open circle symbols are measured O_2 profile data. Depth (z) and J_{O2} are defined with the positive direction into the sediment; height (h) is positive upward from the sediment. (a), Key water- and sediment-side parameters include the diffusive boundary layer (DBL), sediment-water interface (SWI) at z = 0 mm, and depth of the sediment oxic zone (z_{max}). The five methods are defined in panels b–f: (b), direct method; (c), u_* method; (d), curvefit method; (e), zonefit method; and (f), model method. For definitions and units, see Table 1 and supporting method descriptions.

PROFILE, a one-dimensional, numerical procedure for biogeochemical interpretation of sediment porewater profiles (Berg et al. 1998), and AQUASIM, an aquatic system simulation and data analysis software (Reichert 1994), for the zonefit and model methods, respectively. Key components of the vertical O_2 distribution are shown schematically in Fig. 1a. The five methods are illustrated in Fig. 1b–f with additional details provided in text below.

Each method yielded results for either J_{O2} or δ_{DBL}, and then the related parameter (δ_{DBL} or J_{O2}, respectively) was evaluated using Fick's first law of diffusion (Rasmussen and Jørgensen 1992; Lavery et al. 2001; Higashino et al. 2004):

$$J_{O2} = -\varphi D_s \left(\frac{\partial C}{\partial z}\right)_s = -D\left(\frac{\partial C}{\partial z}\right)_w = D\frac{C_{bulk} - C_{SWI}}{\delta_{DBL}} \text{ [mmol m}^{-2}\text{ d}^{-1}\text{]} \quad (2)$$

where φ is sediment porosity (m^3 voids m^{-3} total volume), D_s is the diffusion coefficient for O_2 in sediment (m^2 s^{-1}), D is the diffusion coefficient for O_2 in water (m^2 s^{-1}), and $(\partial C/\partial z)_s$ and $(\partial C/\partial z)_w$ are the O_2 concentration gradients in the sediment at the SWI and in the DBL water immediately above the SWI, respectively (μmol m^{-4}), where depth (z) and corresponding J_{O2} are defined as positive into the sediment with z = 0 mm at the SWI. C_{bulk} is the O_2 concentration in the bulk BBL (μmol L^{-1}), and C_{SWI} is the O_2 concentration at the SWI (μmol L^{-1}), as shown in Fig. 1b. Diffusive transport is hence defined in the sediment by the first expression in Eq. 2 and in the water by the second and third expressions. Values for D were based on $D = 1.97 \times 10^{-9}$ m^2 s^{-1} at 20°C, correcting for temperature using the Stokes-Einstein relationship (Li and Gregory 1974; Arega and Lee 2005). D_s was defined as φD (multiplying by φ provides a correction for tortuosity that ignores other possible higher-order parameterizations; Berg et al. 1998; Glud 2008). This simple tortuosity correction increases the influence of φ on diffusive transport in the sediment ($\varphi D_s = \varphi^2 D$ in the first expression in Eq. 2). The temporal change in O_2 concentration ($\partial C/\partial t$) was evaluated for our series of 14 O_2 profiles by comparing profiles immediately before and after one another and calculating the rate of change in O_2 at each depth. Depth-integrated, areal $\partial C/\partial t$ $(\partial C/\partial t)_a$ was found to be on average ~5% of J_{O2} (Bryant et al. 2010), thus establishing that our profiles were at quasi-steady state.

In the absence of a video camera, SWI estimation was based both on visual interpretation of the profiles individually and as a series (identifying linear DBL regions and on profile kinks related to φ differences between the water and the sediment; Røy et al. 2004) and on assessment of O_2 standard deviations (variation should decrease approaching the SWI due to reduced turbulence fluctuations; Müller et al. 2002; Brand et al. 2007). To account for φ when Eq. 2 was applied to porewater for the sediment-side methods, φ measurements were performed on cores taken from our experiment site (following protocol per Dalsgaard et al. 2000). Additionally, supporting φ predictions were estimated using the numerical model PROFILE (Berg et al. 1998) to analyze φ at a greater depth resolution than possible with core tests (Bryant et al. 2010). Independent average J_{O2} values (J_{O2i}, based on a separate set of microprofiles from the same site and on sediment core φ data) were evaluated via the other four methods (excluding zonefit, i.e., PROFILE), and then a trial-and-error approach was used to estimate depth-specific φ values (which PROFILE uses as an input parameter) required to simulate J_{O2i}. From these evaluations, average φ values of 0.95 in the upper 1 mm and 0.90 at >1 mm below the SWI were obtained and subsequently used in J_{O2} calculations and/or as model input parameters.

J_{O2} estimates obtained using Fick's law (Eq. 2) describe diffusive, not total, O_2 uptake. Hence, influences on nondiffusive O_2 uptake, such as variations in sediment topography, advective porewater flow (typical of porous sediment), and irrigation, are not taken into account (Berg et al. 1998; Jørgensen 2001). Whereas non-diffusive O_2 uptake processes could have been incorporated into some of our analyses (e.g., biodiffusivity and irrigation may be included as input parameters in PROFILE), these effects were neglected for the sake of consistent comparison between methods.

Direct method: J_{O2} was evaluated directly from the linear slope of the DBL as measured via O_2 microsensor (Fig. 1b). The DBL slope $(\partial C/\partial z)_w$ was incorporated into Eq. 2 to obtain J_{O2} and corresponding δ_{DBL}. The third expression in Eq. 2 quantifies δ_{DBL} in terms of an "effective" DBL (Jørgensen and Revsbech 1985), which is obtained by extrapolating $(\partial C/\partial z)_w$ at the SWI to C_{bulk} in the water column. This conceptual definition of the DBL corresponds to the extension of the "true" DBL (based solely on the actual linear region) from the laminar region above the SWI to the mixed bulk region.

u_* method: Because accurate microsensor measurements of the DBL are challenging, an alternative method has been developed that estimates δ_{DBL} as a function of hydrodynamics (Hondzo et al. 2005; O'Connor and Hondzo 2008). This method uses a simplified dimensionless power law for the universal scaling of the vertical O_2 distribution in the bulk water to estimate δ_{DBL} (Fig. 1c). Dimensionless power law scaling was applied to friction velocity (u_*) data derived from ADV velocity series to solve for a nondimensional DBL thickness (δ^+_{DBL}; Hondzo et al. 2005):

$$C^+ = \begin{cases} h^+ \dfrac{\nu}{D} & \text{for } h^+ < \delta^+_{DBL} \\ \delta^+_{DBL} \dfrac{\nu}{D} + \text{BSc}_t \left(\dfrac{1}{\delta^{+2}_{DBL}} - \dfrac{1}{h^{+2}}\right) & \text{for } h^+ \geq \delta^+_{DBL} \end{cases} \text{ [dimensionless]} \quad (3)$$

where C^+, h^+ (= $hu_*\nu^{-1}$), and δ^+_{DBL} are nondimensional parameters for concentration, height, and estimated δ_{DBL} from the power law, respectively. ν is kinematic viscosity (corrected for temperature), B is an integration constant, and Sc_t is the turbulent Schmidt number. We found the product BSc_t to have a functional dependence on the Reynolds number ($Re = u_* \delta_{DBL} \nu^{-1}$) across the series of 14 in situ profiles during our relatively low turbulence conditions. BSc_t and the profile-specific δ^+_{DBL} were used to fit the power law to water-side O_2 profile data immediately above the SWI and evaluate the point at which the two curves defining C^+ ($h^+ < \delta^+_{DBL}$ and $h^+ \geq \delta^+_{DBL}$, as defined in Eq. 3) converge. Once δ^+_{DBL} was estimated (Fig. 1c), it was used to obtain the actual DBL thickness (δ_{DBL}):

$$\delta_{DBL} = \frac{\nu \delta^+_{DBL}}{u_*} \text{ [m]} \quad (4)$$

The corresponding J_{O2} was then calculated using the third expression in Eq. 2.

Curvefit method: This method is based on characterizing the sediment oxic zone with the polynomial $C(z)$ that best fits the profile curve (Fig. 1d) immediately below the SWI (Urban et al. 1997; Glud 2008). A majority of our data were described most accurately by third-order polynomials (profile 6 required a fourth-order equation). Taking the first derivative of $C(z)$, which defines O_2 as a function of depth z, and evaluating this function at the sediment surface (z = 0) yields a constant $(\partial C/\partial z)_s$ that can be incorporated into Eq. 2 to solve for J_{O2} and δ_{DBL}.

Zonefit method: Sediment porewater O_2 data were analyzed using PROFILE (Berg et al. 1998). PROFILE is based on zero-order kinetics and defines zones of constant volumetric O_2 consumption (R_{O2v}; Table 1) to best characterize a sediment O_2 profile (Fig. 1e). At steady state, R_{O2v} may be defined by the derivative of Eq. 2 (Rasmussen and Jørgensen 1992; Glud 2008):

$$R_{O2v} = \frac{\partial}{\partial z}\left(\varphi D_s \left(\frac{\partial C}{\partial z}\right)_s\right) \quad [\text{mmol m}^{-3}\ \text{d}^{-1}] \quad (5)$$

The PROFILE algorithm solves Eq. 5 numerically and reduces the number of zones necessary for obtaining an optimal fit using statistical F-testing. From this statistical analysis, the simplest O_2 consumption–production profile is selected that best models the porewater profile data. We found that the full set of 14 profiles was typically characterized by one or two consumption zones, as also determined by Brand et al. (2008). Our 14 O_2 profiles were used as input data for the numerical procedure. Boundary conditions were defined by O_2 flux and concentration evaluated at the bottom of the profile (J_{O2} = 0 mmol m^{-2} d^{-1} and C = 0 µmol L^{-1}, respectively). Parameters used for the model include D, D_s, and φ as defined above. Irrigation and biodiffusivity effects were assumed to be negligible.

Balancing O_2 transport and consumption results in

$$J_{O2} = \int_0^{z_{max}} R_{O2v}\,dz + \int_0^{z_{max}} \frac{\partial C}{\partial t}\,dz \quad [\text{mmol m}^{-2}\ \text{d}^{-1}] \quad (6)$$

where R_{O2v} (mmol m^{-3} d^{-1}) and the change in O_2 over time ($\partial C/\partial t$, mmol m^{-3} d^{-1}) are integrated over the sediment profile depth to z_{max} (designated as the depth below the SWI where O_2 drops to <3 µmol L^{-1}). Depth-integrated values of R_{O2v} and $\partial C/\partial t$, defined areally by R_{O2a} and $(\partial C/\partial t)_a$, allow for direct comparison with J_{O2} (mmol m^{-2} d^{-1}). J_{O2} values based on PROFILE results were incorporated into Eq. 2 to obtain corresponding δ_{DBL}.

Model method: We used AQUASIM (Reichert 1994) to fit measured O_2 porewater data to the transport-reaction equation:

$$\frac{\partial C}{\partial t} = \frac{\partial}{\partial z}\left(\varphi D_s \frac{\partial C}{\partial z}\right) - \mu \frac{C}{K_{O2} + C} \quad [\text{mmol m}^{-3}\ \text{d}^{-1}] \quad (7)$$

which defines diffusion and consumption by Monod kinetics, where µ is the maximum oxidation rate (mmol m^{-3} d^{-1}) and K_{O2} is the half-saturation constant (µmol L^{-1}). The second expression in Eq. 7 thus characterizes R_{O2v} in terms of Monod kinetics. Monod parameters were obtained using a diffusion-reaction model developed with the sediment module of AQUASIM version 2.1e (Reichert 1994; Brand et al. 2009), which was adapted to include tortuosity effects via D_s. A single set of Monod parameters (µ = 3620 mmol m^{-3} d^{-1} and K_{O2} = 8.0 µmol L^{-1}) was found to characterize steady-state O_2 consumption for the series of 14 O_2 profiles, with C_{SWI} as the only variable. These Monod parameters were subsequently incorporated into a second model run that used C_{bulk} as the upper boundary condition and δ_{DBL} as the sole fitting parameter to reproduce our sediment O_2 data and estimate δ_{DBL} (Fig. 1f) for the full set of profiles. The model method thus allowed us to assess an alternative kinetic approach and to model δ_{DBL} directly from sediment-side data (the zonefit method is based on zero-order O_2 consumption and does not predict δ_{DBL}). J_{O2} was estimated by incorporating AQUASIM-modeled δ_{DBL} into Eq. 2.

Assessment

Dynamic forcing of O_2 distribution—Turbulence-induced variation in our O_2 profile data allowed us to assess the performance and applicability of the different methods for J_{O2} over a range of turbulence levels. The vertical distribution of O_2 on both sides of the SWI (as characterized by δ_{DBL} and z_{max}; Fig. 1a) and J_{O2} were found to be strongly influenced by BBL turbulence during the 12-h measurement period (Fig. 2; Bryant et al. 2010). J_{O2} and δ_{DBL} values shown in Fig. 2 are based on average results of the five methods. Quantified values presented in this study differ slightly (<5% on average) from those in Bryant et al. (2010) owing to a difference in how sediment tortuosity was accounted for (D_s; discussed below), but overall results were not affected. J_{O2} ranged from 6.8 ± 1.9 mmol m^{-2} d^{-1} during peak turbulence (ε = 1.2 × 10^{-8} W kg^{-1}) to 1.0 ± 0.3 mmol m^{-2} d^{-1} during negligible turbulence (ε = 7.8 × 10^{-12} W kg^{-1}), as shown in Fig. 2a. Corresponding variation in u_* is also shown. The DBL was suppressed to a minimum δ_{DBL} of 1.1 ± 0.1 mm, and z_{max} increased to 2.2 mm during peak turbulence (Fig. 2b). When turbulence levels dropped, z_{max} decreased to 0.3 mm and δ_{DBL} increased to the point of becoming technically undefined (Gantzer and Stefan 2003; Røy et al. 2004). However, a conceptual δ_{DBL} was quantified for the sake of comparison during this quiescent period, and a nominal maximum δ_{DBL} of 8.0 ± 2.4 mm was obtained. Average δ_{DBL} and J_{O2} (describing the full O_2 profile set) used for comparative assessment of methods were based on data obtained during active turbulence when a defined δ_{DBL} was maintained (excluding profiles 8 and 9).

Comparison of results—We found J_{O2} and δ_{DBL} estimates from the different methods to be comparable within 20% on average relative to overall change (85%) throughout the experiment (Fig. 3). The range in J_{O2} and δ_{DBL} values obtained per

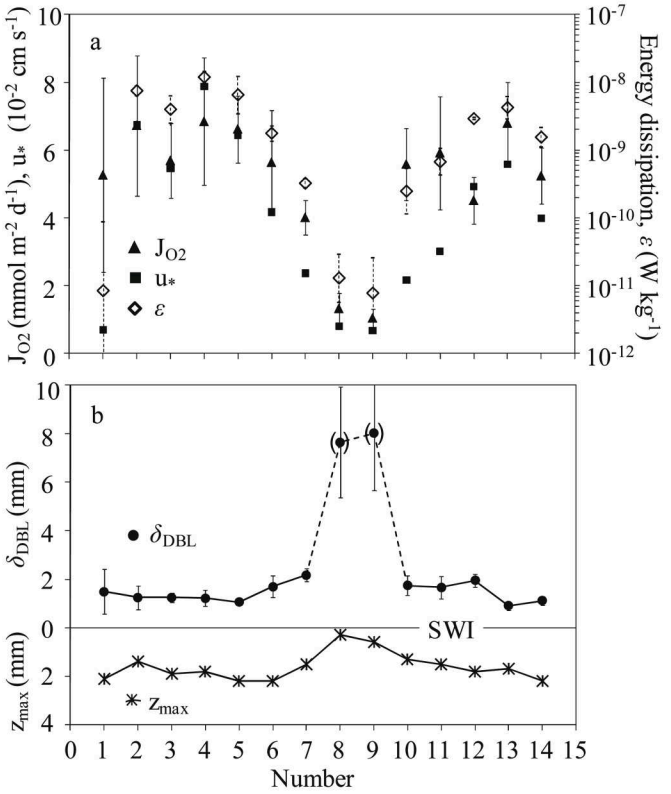

Fig. 2. (a), Time series of J_{O2}, energy dissipation (ε), and friction velocity (u_*) as a function of O_2 profile number. (b), Turbulence-induced variations in the vertical O_2 distribution on both sides of the SWI (as characterized by δ_{DBL} and z_{max}). J_{O2} and δ_{DBL} values shown are the averages from the five methods investigated here (Fig. 1). Modified from Bryant et al. (2010).

profile from the different methods (e.g., the five individual J_{O2} values for profile 5) is relatively small compared to overall temporal variation in averages (e.g., the mean J_{O2} values for profiles 5 and 7). Furthermore, the trend in turbulence-induced changes in J_{O2} (and corresponding δ_{DBL}) is well preserved by all five methods (Figs. 2 and 3). Although there are acknowledged conceptual and methodological difficulties with quantifying δ_{DBL} during quiescent conditions, the methods performed reasonably well during the period of negligible turbulence, with no significant increase in variation relative to average δ_{DBL} (or J_{O2}).

Estimates of J_{O2} obtained with water-side (direct and u_*) methods were consistently higher (and δ_{DBL} estimates correspondingly lower) than those obtained via sediment-side (curvefit, zonefit, and model) methods (Fig. 3). J_{O2} based on water-side data were on average 25% higher than estimates based on sediment-side data, whereas δ_{DBL} values were on average 35% lower (relative to water-side J_{O2} and δ_{DBL}; differences of +1.8 mmol m^{-2} d^{-1} and –0.4 mm, respectively) during active turbulence. Potential reasons for deviation between water- and sediment-side results are discussed below.

To measure the statistical range of results from the five methods, standard deviations (σ) were calculated assuming a normal distribution. Data for σ_{JO2} and σ_{DBL} are shown in Fig. 2. Standard deviations remained relatively low, although variation was observed at certain points during the campaign. During periods of inactive turbulence, increasing δ_{DBL} and decreasing ε led to greater uncertainty and subsequent increases in σ and ε intermittency. Although increased variability in δ_{DBL} and ε was observed during the quiescent period, this was most likely an effect of analysis rather than an indication of poor data quality. Increased variation in J_{O2}, δ_{DBL}, and ε estimates for profile 1 was attributed to equipment settling (Bryant et al. 2010), and hence these data were considered outliers.

Evaluation of each method—In general, each method could be applied to the full profile set for estimations of J_{O2} and δ_{DBL}. Data were more difficult to analyze during periods of negligible turbulence (profiles 8 and 9) because of the disintegration of a measurable DBL (direct method), increased uncertainty in u_* estimates (u_* method), and the breakdown of curvature of sediment porewater O_2 profiles (curvefit, zonefit, and model methods). Furthermore, as with all analytical approaches, each of the methods was found to have both benefits and limitations that had to be considered during analysis and/or assessment. Unless otherwise noted, method results are compared in the following sections using percent difference calculated with respect to average J_{O2} or δ_{DBL}.

Direct method: This method is the most traditional and straightforward (Jørgensen and Revsbech 1985). However, while the O_2 gradient $(\partial C/\partial z)_w$ is relatively simple to measure for the quantification of J_{O2} (Eq. 2), estimating the actual δ_{DBL} directly from O_2 profiles is more problematic due to rapid changes in δ_{DBL} (Røy et al. 2004). The true endpoint of the linear $(\partial C/\partial z)_w$ gradient in the DBL is also often undefined. Jørgensen and Revsbech (1985) addressed this issue by establishing the effective DBL (Eq. 2) for evaluation of δ_{DBL}. Because of the disintegration of the intersection point between the linear DBL region and the constant bulk region in many of our O_2 profiles (observed in profile 14, Fig. 1b), we were unable to precisely capture the true DBL because of turbulence-induced variations in the C_{bulk} endpoint during the ~50-min period required to measure a full profile. Estimating the true δ_{DBL} visually from the strictly linear region of our measured O_2 profiles yielded values 71% less than average δ_{DBL} results (not shown).

Whereas the effective δ_{DBL} approach has been found to overestimate δ_{DBL} (Nishihara and Ackerman 2007; O'Connor et al. 2009), direct method δ_{DBL} was typically slightly lower (11% on average) than mean δ_{DBL} (Fig. 3). Our results are in agreement with those obtained by Jørgensen (2001), who found effective δ_{DBL} to be similar to δ_{DBL} estimated as a function of hydrodynamics using alabaster plate measurements. Although the direct method was relatively easy to apply to our O_2 profiles with comparable results, Nishihara and Ackerman (2007) have suggested a similar but alternate approach using a hyperbolic

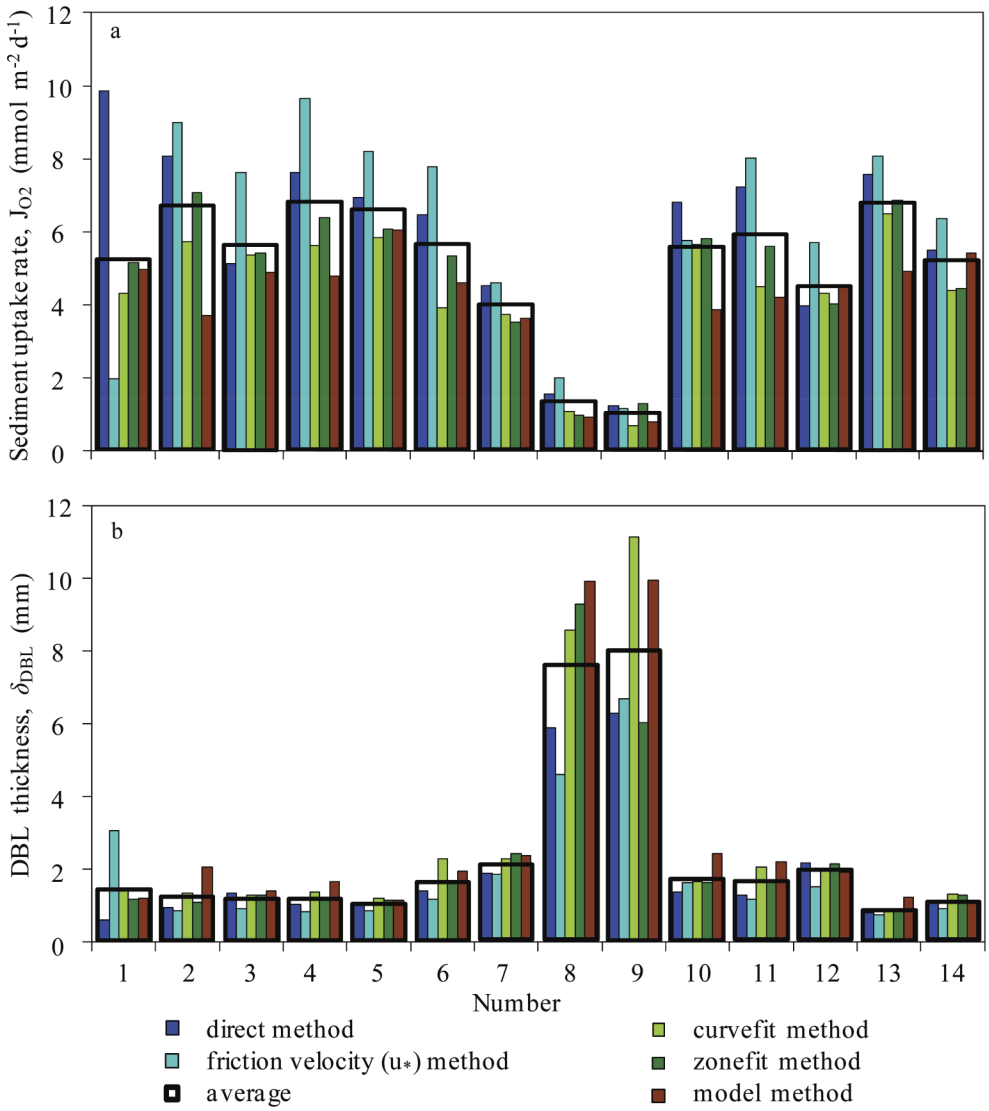

Fig. 3. Comparison of method results for J_{O2} (a) and δ_{DBL} (b) for all 14 profiles. Data for profile 1 considered outliers.

tangent (rather than a straight line) to define $\partial C/\partial z$, which may be optimal for profiles exhibiting nonlinearity in the DBL.

u_* method: While the other four methods are based purely on O_2 microsensor data, the u_* method is unique in that it incorporates water-column hydrodynamics (as characterized by u_*) into the assessment of δ_{DBL}. Estimations of δ_{DBL} from the u_* method are based on both O_2 microsensor and ADV velocity data (used to determine u_*), thus allowing for a more rigorous evaluation of mean δ_{DBL} and J_{O2}. The temporal and spatial scales of u_* and microsensor measurements differed in that u_* data were collected at 32 Hz and determined at 10 cm above the sediment (dm scale), whereas microprofiles were collected subhourly at mm scale across the SWI. However, previous work (Lorke et al. 2003) has established the relationship between δ_{DBL} and velocity at 1 m above the sediment, supporting the use of time-averaged u_* estimates at 10 cm to characterize each microsensor profile.

The u_* method was shown by Hondzo et al. (2005) to predict δ_{DBL} values ~30% lower than the effective δ_{DBL} (i.e., direct method). Similarly, our u_*-based δ_{DBL} estimates were consistently lower than direct method estimates (but within ± 14%; relative to direct method; Fig. 3) and 23% less than average δ_{DBL}. As previously defined, the u_* method estimates δ_{DBL} as a function of the fitting parameter δ^+_{DBL} and Reynolds number–dependent BSc_t using power law scaling of water-side O_2 data. Although the power law easily fit most of our data (e.g., profile 14 in Fig. 1c and profile 3 in Fig. 4a), the fit was less than ideal for several profiles that had increased scatter in bulk water O_2 (e.g., profile 11, Fig. 4b). Because the fits were affected by both δ^+_{DBL} and BSc_t, in several cases the fit was not particu-

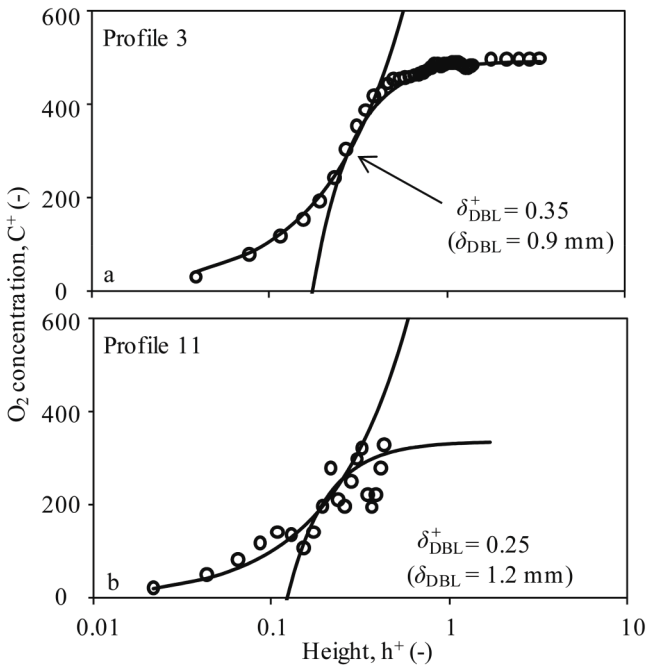

Fig. 4. The universal scaling law (Fig. 1c) could be fitted with the u_* method to a majority of our O_2 profiles, e.g., profile 3 in (a). However, the procedure was not robust for certain profiles, such as profile 11 in (b), and resulted in greater uncertainty in nondimensional δ^+_{DBL}.

larly sensitive to δ^+_{DBL}. These cases were unsystematic, and the resulting combinations varied only slightly from one another, with δ_{DBL} estimations differing by up to ±0.1 mm (<10% of average δ_{DBL} during active turbulence). For these situations, the larger, more conservative value of δ_{DBL} was chosen.

Although J_{O2} and/or δ_{DBL} are commonly assessed as a function of current velocity or u_* data in laboratory studies (Mackenthun and Stefan 1998; Røy et al. 2004; Hondzo et al. 2005), our study is one of the few that have evaluated J_{O2} and δ_{DBL} as a function of turbulence based on in situ current velocity. It is acknowledged that velocity-based approaches may not always be appropriate at low energy (e.g., periodically forced lakes and reservoirs) because turbulence, rather than velocity, controls δ_{DBL} (Lorke et al. 2003). During periods of inactive turbulence, law-of-the-wall theory does not apply (Lorke et al. 2002) and u_* is conceptually not defined. The u_* method may not be as applicable during these periods. Variation between u_*-based estimates and the other methods was not observed to increase during the period of inactive turbulence (profiles 8 and 9, Fig. 3) though, indicating that the u_* method performed adequately even under low-ε conditions.

To further evaluate the validity of estimating δ_{DBL} as a function of in situ velocity during low turbulence and also to test the robustness of the other methods using an independent approach, values of u_*-based δ_{DBL} and average δ_{DBL} were compared to the Batchelor length scale (L_B) for O_2 (Fig. 5). L_B characterizes the minimum length scale of concentration where molecular diffusion begins to reduce concentration gradients (Lorke et al. 2003). Elevated turbulence sustains concentration fluctuations at a smaller scale, which parallels δ_{DBL} behavior. L_B may hence be used as an alternative method of estimating δ_{DBL} as a function of ε, as developed by Hearn and Robson (2000):

$$L_B = 2\pi\left(\frac{\nu D^2}{\varepsilon}\right)^{1/4} \quad [\text{m}] \qquad (8)$$

Although L_B was defined conceptually for open flow rather than for a boundary layer, Lorke et al. (2003) show agreement between L_B and δ_{DBL} despite a substantial spatial gap (~1 m) between ε and O_2 measurements. Taking into account the much smaller spatial gap (~0.1 m) between our measurements, the correlation observed in Fig. 5 further validates δ_{DBL} scaling based on L_B.

Because both L_B and u_* are a function of ε, we specifically evaluated the relationship between L_B and u_* method results for δ_{DBL}. We also compared L_B to average δ_{DBL} (both including all methods and excluding u_* method to isolate the influence of u_* results). As shown in Fig. 5, all three estimates of δ_{DBL} correlate well with L_B (R^2 = 0.95 to 0.96). O'Connor et al. (2009) observed similarity between L_B and u_*-based δ_{DBL} as well, although δ_{DBL} values based on O_2 profile data were found to be overestimated in comparison. Conversely, we observed a strong relationship between L_B and both δ_{DBL} averages (Fig. 5). Our δ_{DBL} estimates based on u_* and purely on O_2 profile data are thus supported by L_B results.

Curvefit method: Mean values of J_{O2} and δ_{DBL} based on curvefit results were within ~10% of the average (Fig. 3). Fitting curves to porewater profiles has been used effectively to quantify kinetic rates of O_2 consumption and corresponding O_2 fluxes in previous work (Nielsen et al. 1990). Ideally, derivatives of the best-fitting curve can be used to evaluate J_{O2} and R_{O2v} (Rasmussen and Jørgensen 1992). Zero-order kinetics are characterized by second-order polynomials and first-order kinetics by exponential equations (Bouldin 1968). Third-order polynomials, though, were found to best fit a majority of the sediment O_2 profiles in our data set. It was also difficult to fit a single curve throughout the full depth of the oxic zone for many of our profiles. Therefore, emphasis was placed on precisely fitting the region of the curve immediately at the SWI and incorporating the derivative at z = 0 into Eq. 2. That our data could not be defined by a single second-order polynomial indicates that consumption rates were dependent on depth, which was further explored using multiple zero-order consumption zones (zonefit method) and Monod kinetics (model method).

Zonefit method: The zonefit method yielded mean J_{O2} and δ_{DBL} estimates that were 5% lower and 2% higher, respectively, than average values (Fig. 3). The approach used for this method, based on splining multiple second-order polynomials together to best fit a sediment O_2 profile, is advantageous because it does not assume complex reaction laws and assigns zero-order kinetic rates to as many different zones as needed to

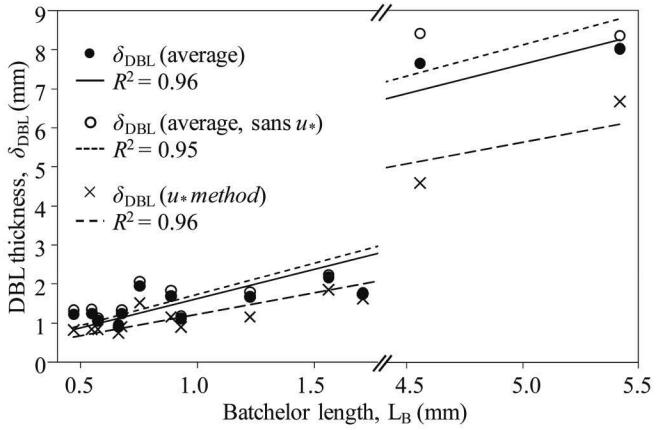

Fig. 5. Relationship between O_2 Batchelor length scale (L_B) and δ_{DBL}. Estimates of δ_{DBL} based on the u_* method and the average (with and without u_* method results) are compared to L_B (Eq. 8). Profile 1 outlier data are excluded.

adequately reproduce the measured profile. The use of multiple zones allows for a good fit to be obtained even for atypical profiles (Maerki et al. 2006). Key benefits of the PROFILE numerical model include simplicity and broad-ranging applicability. PROFILE may be used for any solute that is produced or consumed. Also, variations in φ, biodiffusion, and irrigation may be easily incorporated into PROFILE as a function of profile depth. As with most numerical modeling work, the zonefit method (as well as the model method) was initially labor intensive. However, once the PROFILE model is set up, PROFILE runs quickly and is faster than AQUASIM (model method).

Results from both the zonefit and model methods were used to infer additional information about the sediment. In addition to evaluating J_{O2} and δ_{DBL}, both of these methods were used to predict how O_2 consumption varied as a function of depth and O_2 availability within the sediment oxic zone. Variations in PROFILE-predicted R_{O2v} and zero-order O_2 consumption zones in response to turbulence-induced changes in J_{O2} and subsequent O_2 availability are shown in green in Fig. 6 (discussed further below). Although $\partial C/\partial t$ was minimal (5% on average) for our quasi–steady-state system, zone-specific R_{O2v} values in Fig. 6 were corrected for $\partial C/\partial t$ by establishing a mass balance (Eq. 6) between O_2 consumption zones over the depth of each profile.

Model method: The model method evaluates both sides of the SWI simultaneously to directly estimate δ_{DBL}. Whereas the model we used, formulated in the sediment module of AQUASIM, is largely based on fitting porewater O_2 data and defining sediment O_2 consumption (hence, considered a sediment-side method), water-side data (C_{bulk}) were also used to define the upper boundary condition (the lower boundary condition was defined by zero flux). Because our diffusion-reaction model provided δ_{DBL} as an output parameter for a steady-state solution, we were thus able to estimate δ_{DBL} directly from porewater and bulk water data. Alternatively, the curvefit and zonefit methods evaluate J_{O2} from porewater data and then δ_{DBL} was calculated via Eq. 2. On average, model method estimations of δ_{DBL} were found to be 21% higher (J_{O2} correspondingly 20% lower) than the overall mean (Fig. 3). AQUASIM-estimated δ_{DBL} are delineated by the red water-side fit lines shown in Fig. 6.

Monod parameters estimated by AQUASIM to best characterize our O_2 profile data and model δ_{DBL} were also used to evaluate how R_{O2v} changed as a function of depth and time (Fig. 6). Although we incorporated only a single Monod formulation in this study, the sediment module of AQUASIM can be used to implement process-based sediment reaction models with more complex kinetics (e.g., Brand et al. 2009). The AQUASIM model can also be used to predict variation in O_2 consumption pathways if several terminal electron acceptors which compete for O_2 are considered as parameters in the model.

Discussion

Water-side versus sediment-side—The general applicability of each of the methods is established by the fact that differences between method results are small relative to overall variation in J_{O2} and δ_{DBL}. Although some deviation between water- and sediment-side estimates was observed, trends in J_{O2} and δ_{DBL} were sufficiently captured by both water- and sediment-side methods (Figs. 2 and 3). Nevertheless, this deviation warrants further evaluation. As previously mentioned, water-side methods yielded comparable but consistently higher J_{O2} and correspondingly lower δ_{DBL} than sediment-side methods (differences of 1.8 mmol m^{-2} d^{-1} [25%] and 0.4 mm [35%] on average, respectively). Our results are comparable to those obtained in a study of total and diffusive O_2 uptake in marine sediment by Rabouille et al. (2003), which found that while total O_2 uptake was in close agreement with J_{O2} based on the interface gradient (direct method), PROFILE-predicted (zonefit method) J_{O2} was 20% less. Relative to the differences observed between our water- and sediment-side results, variation is much smaller within the water-side group (±7%) and the sediment-side group (±10%) as shown in Table 2 and Fig. 3. Deviation between water- and sediment-side estimates occurs throughout the full data set for our 12-h experiment with no evident correlation to turbulence and corresponding u_* (Table 2; Fig. 2). SWI identification, methodological issues, assumptions made on sediment properties, and localized sediment O_2 transport and consumption processes may have contributed to the difference in water- and sediment-side estimates.

Estimation of the SWI location is not trivial and may have influenced both water- and sediment-side results. Whereas the u_* method evaluates the water O_2 profile up to several mm above the SWI and the zonefit and model methods assess the full porewater O_2 profile, the direct and curvefit methods are focused immediately on changes in $(\partial C/\partial z)_w$ and $(\partial C/\partial z)_s$ at the SWI and are thus much more sensitive to the SWI location (Rabouille et al. 2003). If, for example, the actual SWI location was higher than estimated, $(\partial C/\partial z)_s$ would have been underestimated and $(\partial C/\partial z)_w$ overestimated in some profiles.

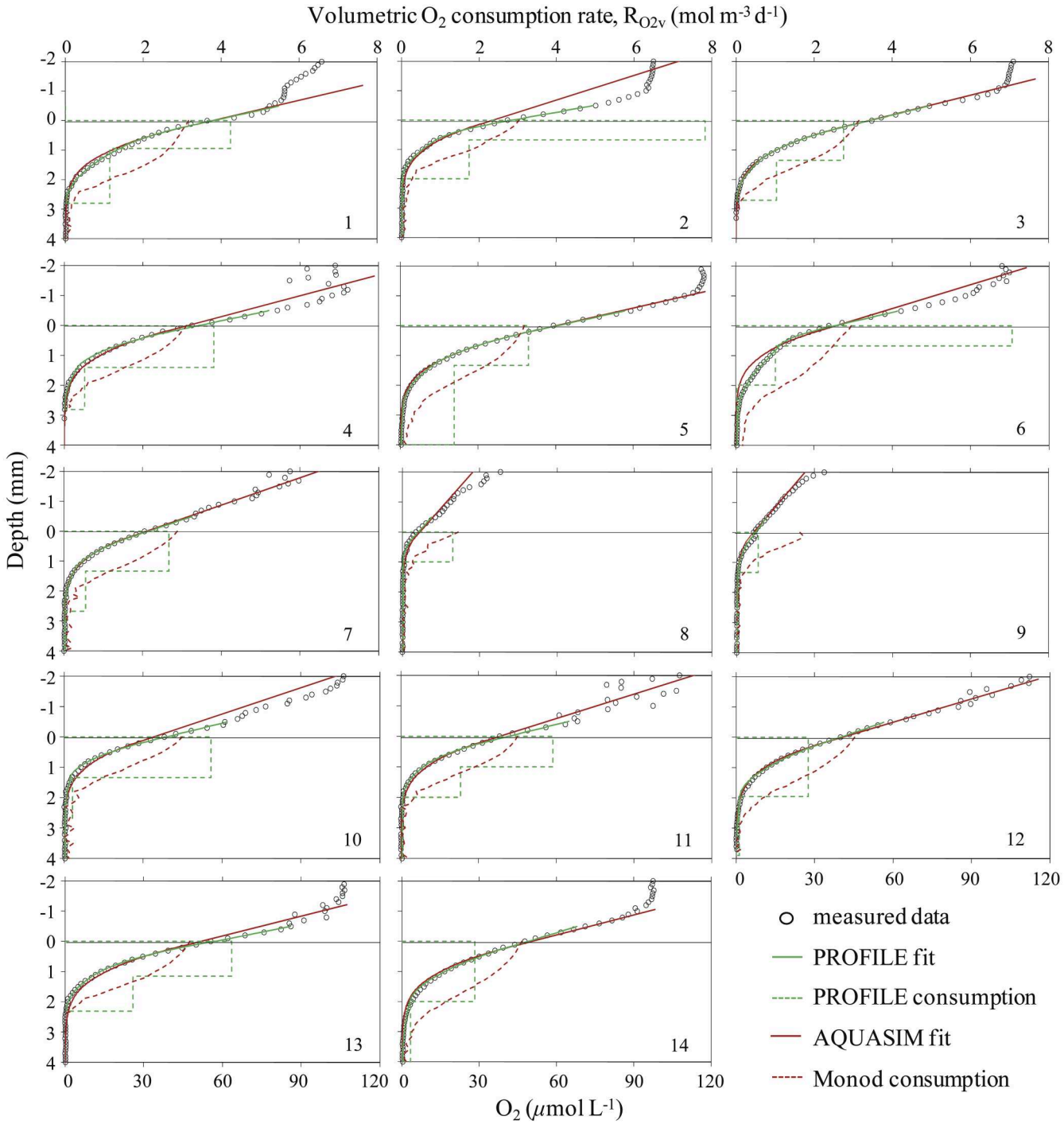

Fig. 6. Volumetric O_2 consumption rate R_{O2v} as predicted by the zonefit method (PROFILE; based on zero-order kinetics; green) and the model method (AQUASIM; based on Monod kinetics; red). Model fits designated by solid lines and model-based predictions of sediment O_2 consumption designated by dashed lines. SWI located at depth z = 0 mm.

Water-side estimates obtained via the direct method could have been influenced by difficulties associated with quantifying δ_{DBL} directly from O_2 profiles. Recent work has suggested that it is inadequate to classify the DBL as quiescent because δ_{DBL} varies continuously as a function of BBL currents (Røy et al. 2004; O'Connor and Hondzo 2008). Brand et al. (2009), however, showed that the use of a quiescent DBL is a valid model for the study of O_2 dynamics over time scales of several minutes to hours (i.e., the 8-h seiche cycle inducing variations in turbulence observed during this study) and that high-fre-

Table 2. Average sediment oxygen uptake rate (J_{O2}), average diffusive boundary layer thickness (δ_{DBL}), and corresponding distributions of results (± standard deviation σ) based on estimates from all five methods, water-side approaches (direct and u_*), and sediment-side approaches (curvefit, zonefit, and model). The percent difference between water- and sediment-side averages (relative to water-side) shows that water-side estimates of J_{O2} were consistently higher and δ_{DBL} consistently lower than sediment-side estimates.

	Average J_{O2}, mmol m^{-2} d^{-1}				Average δ_{DBL}, mm			
Profile number	All methods	Water-side	Sediment-side	Difference, %	All methods	Water-side	Sediment-side	Difference, %
1	5.3 ± 2.9	5.9 ± 5.6	4.8 ± 0.4	+19	1.5 ± 0.9	1.8 ± 1.7	1.3 ± 0.1	+32
2	6.7 ± 2.1	8.5 ± 0.7	5.5 ± 1.7	+35	1.2 ± 0.5	0.9 ± 0.1	1.5 ± 0.5	–66
3	5.7 ± 1.1	6.4 ± 1.8	5.2 ± 0.3	+18	1.2 ± 0.2	1.1 ± 0.3	1.3 ± 0.1	–18
4	6.8 ± 1.9	8.6 ± 1.4	5.6 ± 0.8	+35	1.2 ± 0.3	0.9 ± 0.2	1.4 ± 0.2	–54
5	6.6 ± 1.0	7.6 ± 0.9	6.0 ± 0.1	+21	1.1 ± 0.1	0.9 ± 0.1	1.2 ± 0.0	–26
6	5.6 ± 1.5	7.1 ± 0.9	4.6 ± 0.7	+35	1.7 ± 0.4	1.3 ± 0.2	2.0 ± 0.3	–55
7	4.0 ± 0.5	4.6 ± 0.1	3.6 ± 0.1	+20	2.2 ± 0.3	1.9 ± 0.0	2.4 ± 0.1	–26
8	1.3 ± 0.5	1.8 ± 0.3	1.0 ± 0.1	+44	7.6 ± 2.3	5.2 ± 0.9	9.2 ± 0.7	–77
9	1.0 ± 0.3	1.2 ± 0.1	0.9 ± 0.3	+23	8.0 ± 2.4	6.5 ± 0.3	9.0 ± 2.7	–40
10	5.6 ± 1.1	6.3 ± 0.8	5.1 ± 1.1	+19	1.7 ± 0.4	1.5 ± 0.2	1.9 ± 0.5	–26
11	5.9 ± 1.7	7.6 ± 0.5	4.8 ± 0.7	+37	1.7 ± 0.5	1.2 ± 0.1	2.0 ± 0.3	–62
12	4.5 ± 0.7	4.8 ± 1.2	4.3 ± 0.2	+12	2.0 ± 0.3	1.8 ± 0.5	2.0 ± 0.1	–10
13	6.8 ± 1.2	7.8 ± 0.3	6.1 ± 1.0	+22	0.9 ± 0.2	0.8 ± 0.0	1.0 ± 0.2	–31
14	5.2 ± 0.8	5.9 ± 0.6	4.8 ± 0.6	+20	1.1 ± 0.2	1.0 ± 0.1	1.2 ± 0.1	–25
Average[a]	5.8 ± 1.2	6.9 ± 0.8	5.1 ± 0.7	+25	1.5 ± 0.3	1.2 ± 0.2	1.6 ± 0.2	–36

[a]Time-averaged δ_{DBL} and J_{O2} (characterizing the O_2 profile series) used for comparative assessment are based on data obtained during active turbulence (thus excluding profiles 8 and 9). However, including data from the quiescent period typically affected average J_{O2} and δ_{DBL} comparisons by <5%. Outlier profile 1 data also excluded.

quency fluctuations have no significant effect on time-averaged flux. Although no defined trends were observed between turbulence and deviation in direct and u_* method results, conceptual issues with quantifying ε and u_* during low turbulence conditions may also have been a factor.

Equipment-induced modification of hydrodynamics likely had a minimal effect on observed variation in water- and sediment-side estimates. The open structure of the microprofiler frame was designed to have negligible influence on hydrodynamics, and the ADV was located several meters away from the microprofiler. Microsensor compression of the DBL, which has been attributed to flow acceleration around the electrode shaft (Glud et al. 1994; Glud 2008), may have affected measurements. Although changes in our series of sediment O_2 profiles due to profiling in the same location were not discerned (as discussed in "Materials and procedures"), repeated profiling and subsequent localized changes in sediment properties (e.g., φ variations, creation of oxic channels) and reaction rates could affect sediment-side J_{O2}, particularly in systems with lower φ (e.g., biofilms, highly cohesive sediment), longer O_2 residence times, and/or when using larger-diameter sensors.

Sediment O_2 transport processes were defined for sediment-side methods using experimentally obtained and/or assumed parameters (e.g., φ and biodiffusivity, respectively). The relatively high degree of uncertainty in these sediment parameters (P. Berg, pers. comm.) and subsequent effects on J_{O2} and δ_{DBL} estimations (discussed below) could have been a source of deviation between water- and sediment-side results. Quantifying diffusive transport and the relationship between φ and D_s in sediment is complicated by the heterogeneous nature of typical sediment matrices (Glud 2008). Previous work has shown that the influence of tortuosity on diffusion may be negligible in freshwater sediment, particularly near the SWI where φ approaches unity (Maerki et al. 2004). Our measured sediment φ was ≥0.95 in the upper sediment, and only slight changes in O_2 profile slope were evident at the SWI. For these reasons, we did not correct for tortuosity in curvefit and model method analyses in Bryant et al. (2010). PROFILE (zonefit method), however, requires tortuosity to be defined via input parameter D_s. To maintain consistency when evaluating the methods, D_s (which we parameterized as $D_s = \varphi D$) was incorporated into all sediment-side analyses in this comparative study. Of the three possible D_s parameterizations defined in PROFILE (Berg et al. 1998) and also relative to other published D_s definitions for cohesive sediment (Glud 2008), this parameterization minimized tortuosity effects. Accounting for tortuosity in all sediment-side analyses changed results by a factor of φ^2 or ~5% (with $\varphi = 0.95$), which directly reflects the additional influence of φ due to the tortuosity correction ($\varphi D_s = \varphi^2 D = 0.90D$ per Eq. 2 compared with $\varphi D = 0.95D$ per Bryant et al. 2010). Using a higher-order correction for tortuosity would affect results to an even greater extent (e.g., $D_s = \varphi^2 D$ would decrease J_{O2} by a fac-

tor of φ^3 or 10%), which highlights the sensitivity of these analyses to sediment property parameterization.

To further equate method comparisons and simplify assumptions made for unknown input parameters, bioturbation and irrigation effects were assumed to be negligible. However, bioturbation (i.e., the mixing of solutes and solids in sediment due to fauna movement; Berg et al. 2001) has been shown to increase J_{O2} estimates by up to 85% based on total sediment O_2 uptake in marine sediment (Glud 2008). Enhanced O_2 flux into the sediment due to these processes would not have been accounted for in J_{O2} estimates based solely on diffusive transport (as our results were; Eq. 2). *Chironomidae sp*. and *Oligochaeta sp*. were found in sediment cores obtained from our experiment site (data not shown), and bioturbators have also been observed in similar systems (e.g., Lake Sempach; Bürgi and Stadelmann 2002). To investigate the influence of bioturbation (characterized via biodiffusivity, D_b), we performed a follow-up analysis using PROFILE that evaluated D_b required to estimate J_{O2} equivalent to water-side J_{O2}. Average J_{O2} initially predicted by PROFILE via the zonefit method was 5.5 mmol m^2 d^{-1} (input D_b = 0 m^2 s^{-1}). By changing the D_b value used to model our O_2 porewater data, we found that a D_b of 5.0×10^{-10} m^2 s^{-1} increased J_{O2} to the average water-side J_{O2} value (6.9 mmol m^2 d^{-1}; Table 2). These results are similar to work by Berg et al. (2001), who showed that including bioturbation in their O_2 flux evaluation caused J_{O2} to increase from 4.1 mmol m^{-2} d^{-1} (D_b = 0 m^2 s^{-1}) to 6.5 mmol m^{-2} d^{-1} ($D_b = 4.6 \times 10^{-10}$ m^2 s^{-1}). Uncertainties in assumed sediment parameters could therefore have contributed to differing sediment- and water-side results.

In addition to difficulties associated with defining bulk sediment properties, sediment-side evaluations of J_{O2} may be complicated by localized sediment O_2 transport and consumption processes that may not be accurately characterized by O_2 porewater data. Variable sediment microtopography effects, bioturbation, and irrigation can have site-specific effects on diffusive O_2 transport (Jørgensen and Des Marais 1990; Røy et al. 2002; Rabouille et al. 2003). Small-scale heterogeneity in mineralization of newly deposited organic matter at the sediment surface (Zhang et al. 1999; Lewandowski et al. 2002) and O_2 consumption via benthic fauna (Krantzberg 1985; Polerecky et al. 2006; Lewandowski et al. 2007) can also cause localized variation in sediment O_2 uptake. Glud et al. (2009) have shown that small-scale disparities in labile organic matter distribution can result in significant variability in surface sediment O_2 concentrations and localized "hot spots" of benthic O_2 consumption.

The effect of spatially heterogeneous O_2 uptake would not have been accurately characterized by microsensor porewater measurements if localized O_2 uptake within the sediment occurred near but did not directly influence the O_2 microprofile site (Brand et al. 2008). Water-side estimates remain relatively unaffected by small-scale variation in site-specific sediment processes owing to the homogenizing effect of turbulence on C_{bulk} and O_2 levels in the DBL (e.g., the spatial scale of averaging within the BBL for an 8-h seiche with a flow of 3 cm s^{-1} is ~1 km; within the DBL, an average flow of 1 cm s^{-1} and O_2 residence time of 10 min would influence a scale of ~6 m). Water-side estimates may therefore be more representative of a larger areal "footprint" than sediment-side estimates (Berg et al. 2007b; O'Connor and Hondzo 2008). If considerable localized sediment O_2 uptake processes were occurring near our O_2 microsensor but were not captured in profile data, then J_{O2} estimates based on water-column data would be higher than site-specific, porewater-based J_{O2}. Our sediment O_2 profiles are parabolic in shape with no kinks or shifts in the curvature (Jørgensen and Revsbech 1985), and deviation between water- and sediment-side J_{O2} estimates is relatively small, indicating that the influence of localized O_2 uptake processes on the vertical O_2 distribution was likely insignificant.

The eddy correlation method has proven to be a viable and noninvasive approach for estimating total O_2 flux that does not disturb in situ conditions (hydrodynamic or sediment) and is not influenced by localized O_2 consumption processes (Berg et al. 2003; Brand et al. 2008; Lorrai et al. 2010). Although we did attempt eddy correlation measurements for this study to compare total O_2 flux to diffusive J_{O2} estimates, we were unfortunately unable to obtain a quality eddy correlation data set due to equipment problems.

Sediment O_2 consumption—Further evaluation of porewater O_2 data provided beneficial information on O_2 consumption processes within the sediment that could not have been discerned from a water-side assessment. Because we were unable to fully characterize the profiles using second-order polynomial or exponential equations, zero- and first-order kinetic models could not be directly applied to our data set using the curvefit method. However, zero-order (multi-zone) and Monod kinetic models were applied using the zonefit and model methods, respectively. Based on these results, variations in R_{O2v} as a function of depth and time are shown in Fig. 6 (zonefit [PROFILE] in green; model [AQUASIM] in red). Sediment O_2 consumption during turbulent periods was typically characterized by PROFILE with two consumption zones (Fig. 6). R_{O2v} was consistently higher in the upper region of the sediment (immediately below the SWI) and decreased significantly with depth during periods of active turbulence (e.g., profiles 2–5 and 11–14; Fig. 2a). Conversely, during the period when turbulence was negligible (profiles 8 and 9), R_{O2v} decreased and O_2 consumption was characterized by a single zone. R_{O2v} values based on AQUASIM-estimated Monod kinetics and the corresponding regions of sediment O_2 consumption generally followed the same trend as the R_{O2v} values and zero-order O_2 consumption zones predicted by PROFILE (Fig. 6). Corresponding profile-specific R_{O2a} estimates based on zonefit and model method results were within ~20% on average (data not shown). Similar characterization of sediment O_2 consumption by multiple kinetic models verifies results from both

methods and also emphasizes the influence that turbulence-induced changes in O_2 availability had on R_{O2} (Fig. 6). Whereas zero-order kinetics are frequently used to characterize sediment O_2 consumption independent of O_2 concentration (Rasmussen and Jørgensen 1992; Jørgensen and Boudreau 2001), it has been shown that R_{O2v} can become dependent on O_2 concentration under limiting conditions such as the relatively low sediment O_2 levels observed during our study (Santschi et al. 1990; Berg et al. 2003; Bryant et al. 2010).

Our results, which show elevated O_2 consumption in the upper sediment in response to increased O_2 availability at the SWI, indicate water-side control of J_{O2} with the potential sediment O_2 demand surpassing the amount of O_2 supplied to the sediment (O'Connor and Harvey 2008). Sediment O_2 consumption can alternatively be the rate-limiting step to mass transport in physiologically active systems experiencing moderate flow (Nishihara and Ackerman 2009). We observed R_{O2v} to decrease with depth, suggesting that R_{O2v} may have been dominated by mineralization of newly deposited organic matter at the sediment surface (Santschi et al. 1990; Zhang et al. 1999). Similarly, Brand et al. (2009) showed that Alpnach sediment can be sufficiently modeled as a uniform layer of organic matter with a high intrinsic capacity for O_2 uptake and transport-limited J_{O2}. R_{O2v} has been found to increase with depth in environments (e.g., oligotrophic) where re-oxidation of reduced compounds dominates O_2 consumption (Glud et al. 2007; Jørgensen and Boudreau 2001).

Comments and recommendations

Although analogous results were obtained from all five methods, each of the methods had advantages and disadvantages that may affect applicability for specific experiments. The direct method is the least complicated, although rapid variations in the DBL may have influenced effective δ_{DBL} estimates during the ~50-min measurement period of each profile. The u_* method incorporates velocity as an independent variable and provided comparable results; however, we had difficulties in fitting the power law to the full set of profiles, particularly for profiles exhibiting scatter in bulk O_2 data. Water-side approaches may lose validity during periods of weak turbulence due to disintegration of the DBL and/or insignificant u_* values, but the strong correlation between L_B and δ_{DBL} estimates indicates that velocity-based estimates of δ_{DBL} can be adequate even for low turbulence. Our results also support the use of L_B to estimate δ_{DBL} as a function of hydrodynamics, which is somewhat unexpected considering that ε becomes undefined during inactive periods.

As with the direct method, the curvefit method proved to be relatively uncomplicated. Because we could not characterize our sediment profiles with a single curve, we essentially applied a sediment-side version of the direct method to O_2 porewater data. Although sediment φ and tortuosity must be accounted for, the O_2 profile immediately below the SWI may be less variable (and thus easier to measure) than the DBL in many environments. Therefore, the curvefit method may be optimal as a straightforward J_{O2} estimation when porewater data are available and detailed information on variation in R_{O2} within the sediment is not desired.

Estimates of J_{O2} and δ_{DBL} from the zonefit method were the closest to average values (within 5% and 2%, respectively). Although the zonefit and model methods were more laborious than the other methods, significant information on how O_2 consumption varied with sediment depth was obtained. Advantages of the zonefit method include the direct analytical approach, the relative ease in which the PROFILE model can be set up and applied, and the broad applicability of PROFILE. However, PROFILE does not include dynamic processes and thus predictions of how J_{O2} and other fluxes vary over time are dependent on the number of profiles available to characterize transient conditions. A benefit of the AQUASIM diffusion-reaction model used for the model method is that it can predict how the vertical O_2 distribution and corresponding SWI fluxes are affected by dynamic conditions (e.g., variations in δ_{DBL}; Brand et al. 2009). This is especially advantageous if only a few profiles and/or proxies for δ_{DBL} (e.g., u_*, ε) are available. Fortunately, we obtained a sufficient number of profiles over a brief time period to use PROFILE to evaluate the vertical O_2 distribution and J_{O2} under dynamic conditions. If our data set had not been as extensive, AQUASIM may have been the more appropriate approach.

During this study, a direct correlation between O_2 availability in the sediment and sediment O_2 consumption was observed (as characterized by J_{O2} and R_{O2}, respectively) indicating that O_2 dynamics were water-side controlled in our highly-organic, cohesive sediment. However, O'Connor et al. (2009) showed that in porous sediment where J_{O2} is sediment-side controlled, C_{SWI} may approach C_{bulk} under highly turbulent conditions. In this case, J_{O2} would be inaccurately estimated as zero via Eq. 2. This highlights that the approaches evaluated in this study are applicable only to diffusive J_{O2}, as controlled by the driving forces ($C_{bulk} - C_{SWI}$) and δ_{DBL}, and would not apply in systems dominated by advective transport.

In conclusion, by evaluating the robustness of five established methods used to analyze J_{O2} and δ_{DBL} at the molecular level, we show that estimations of these parameters are not strongly dependent on the method chosen. Increased correlation was observed in method results based on the same side of the SWI. Although water-side estimates of J_{O2} were observed to be consistently higher (and estimates of δ_{DBL} lower) than sediment-side estimates, turbulence-induced variations in J_{O2} and δ_{DBL} were reliably characterized by all five methods. All methods were found to have both benefits and limitations. Water-side estimates of J_{O2} and δ_{DBL} typically displayed increased variability due to rapid turbulent fluctuations, the influence of nondiffusive O_2 uptake processes (e.g., bioturbation), and spatial-averaging effects over a broader area. Conversely, while sediment-side measurements may be more robust as the sediment is frequently a less transient environment than the BBL, accurately characterizing sediment

properties and $(\partial C/\partial z)_s$, which often changes more rapidly with depth than $(\partial C/\partial z)_w$, presents additional difficulties.

Our results reveal that the effectiveness and applicability of each of the methods depend largely on available data on the vertical O_2 distribution (e.g., data set sufficiently defining effects of dynamic conditions) and sediment properties (e.g., φ and D_b) and on information desired from the experiment (e.g., J_{O2} and/or R_{O2}). Observed variation in water- and sediment-side estimates of J_{O2} does emphasize that, by focusing solely on a single side of the SWI, difficulties in analyzing relatively transient water-side data and/or effects of site-specific sediment porewater data could potentially result in significantly different interpretations of sediment-water flux. By evaluating the vertical O_2 distribution on both sides of the SWI, a comprehensive assessment of the balance between in situ hydrodynamic and localized sediment O_2 consumption processes and the resulting J_{O2} and R_{O2} is attained.

References

Arega, F., and J. H. W. Lee. 2005. Diffusional mass transfer at sediment-water interface of cylindrical sediment oxygen demand chamber. J. Environ. Eng.-ASCE 131:755-766 [doi:10.1061/(ASCE)0733-9372(2005)131:5(755)].

Baker, M. A., and C. H. Gibson. 1987. Sampling turbulence in the stratified ocean: Statistical consequences of strong intermittency. J. Phys. Oceanogr. 17:1817-1836 [doi:10.1175/1520-0485(1987)017<1817:STITSO>2.0.CO;2].

Berg, P., N. Risgaard-Petersen, and S. Rysgaard. 1998. Interpretation of measured concentration profiles in sediment pore water. Limnol. Oceanogr. 43:1500-1510 [doi:10.4319/lo.1998.43.7.1500].

———, S. Rysgaard, P. Funch, and M. K. Sejr. 2001. Effects of bioturbation on solutes and solids in marine sediments. Aquat. Microb. Ecol. 26:81-94 [doi:10.3354/ame026081].

———, H. Røy, F. Janssen, V. Meyer, B. B. Jørgensen, M. Huettel, and D. de Beer. 2003. Oxygen uptake by aquatic sediments measured with a novel non-invasive eddy-correlation technique. Mar. Ecol. Prog. Ser. 261:75-83 [doi:10.3354/meps261075].

———, D. Swaney, S. Rysgaard, B. Thamdrup, and H. Fossing. 2007a. A fast numerical solution to the general mass-conservation equation for solutes and solids in aquatic sediments. J. Mar. Res. 65:317-343.

———, H. Røy, and P. L. Wiberg. 2007b. Eddy correlation flux measurements: The sediment surface area that contributes to the flux. Limnol. Oceanogr. 52:1672-1684.

Bouldin, D.R. 1968. Models for describing the diffusion of oxygen and other mobile constituents across the mud-water interface. J. Ecol. 56:77–87 [doi:10.2307/2258068].

Boudreau, B. P. 2001. Solute transport above the sediment-water interface, p. 104-126. *In* B. P. Boudreau and B. B. Jørgensen [eds.], The benthic boundary layer: Transport processes and biogeochemistry. Oxford University Press.

Brand, A., and others. 2007. Microsensor for in situ flow measurements in benthic boundary layers at submillimeter resolution with extremely slow flow. Limnol. Oceanogr. Methods 5:185-191.

———, D. F. McGinnis, B. Wehrli, and A. Wüest. 2008. Intermittent oxygen flux from the interior into the bottom boundary of lakes as observed by eddy correlation. Limnol. Oceanogr. 53:1997-2006.

———, C. Dinkel, and B. Wehrli. 2009. Influence of the diffusive boundary layer on the solute dynamics in the sediments of a seiche-driven lake: A model study. J. Geophys. Res. 114:G01010 [doi:10.1029/2008JG000755].

Bryant, L. D., C. Lorrai, D. F. McGinnis, A. Brand, A. Wüest, and J. C. Little. 2010. Variable sediment oxygen uptake in response to dynamic forcing. Limnol. Oceanogr. 55:950-964.

Bürgi, H., and P. Stadelmann. 2002. Change of phytoplankton composition and biodiversity in Lake Sempach before and during restoration. Hydrobiologia 469:33-48 [doi:10.1023/A:1015575527280].

Dalsgaard, T. [ed.], and others. 2000. Protocol handbook for NICE – Nitrogen Cycling in Estuaries: A project under the EU research programme: Marine Science and Technology (MAST III). National Environmental Research Institute, Silkeborg, Denmark. http://www2.dmu.dk/LakeandEstuarineEcology/nice/NICE_handbook.pdf.

Epping, E. H. G., and W. Helder. 1997. Oxygen budgets calculated from in situ microprofiles for Northern Adriatic sediments. Cont. Shelf Res. 17:1737-1764 [doi:10.1016/S0278-4343(97)00039-3].

Gantzer, C. J., and H. G. Stefan. 2003. A model of microbial activity in lake sediments in response to periodic water-column mixing. Water Res. 37:2833-2846 [doi:10.1016/S0043-1354(03)00110-6].

Glud, R. N. 2008. Oxygen dynamics of marine sediments. Mar. Biol. Res. 4:243-289 [doi:10.1080/17451000801888726].

———, J. K. Gundersen, N. P. Revsbech, and B. B. Jørgensen. 1994. Effects on the benthic diffusive boundary layer imposed by microelectrodes. Limnol. Oceanogr. 39:462-467 [doi:10.4319/lo.1994.39.2.0462].

———, P. Berg, H. Fossing, and B. B. Jørgensen. 2007. Effect of the diffusive boundary layer on benthic mineralization and O_2 distribution: A theoretical model analysis. Limnol. Oceanogr. 52:547-557 [doi:10.4319/lo.2007.52.2.0547].

———, H. Stahl, P. Berg, F. Wenzhöfer, K. Oguri, and H. Kitazato. 2009. In situ microscale variation in distribution and consumption of O_2: A case study from a deep ocean margin sediment (Sagami Bay, Japan). Limnol. Oceanogr. 54:1-12.

Grant, H. L., R. W. Stewart, and A. Moilliet. 1962. Turbulence spectra from a tidal channel. J. Fluid Mech. 12:241-268 [doi:10.1017/S002211206200018X].

Gundersen, J. K., and B. B. Jørgensen. 1990. Microstructure of diffusive boundary layers and the oxygen uptake of the sea floor. Nature 345:604–607 [doi:10.1038/345604a0].

Hearn, C. J., and B. J. Robson. 2000. Modelling a bottom diurnal boundary layer and its control of massive alga blooms in an estuary. Appl. Math. Mod. 24:843–859 [doi:10.1016/S0307-904X(00)00020-2].

Higashino, M., C. J. Gantzer, and H. G. Stefan. 2004. Unsteady diffusional mass transfer at the sediment/water interface: Theory and significance for SOD measurement. Water Res. 38:1-12 [doi:10.1016/j.watres.2003.08.030].

Hondzo, M., T. Feyaerts, R. Donovan, and B. L. O'Connor. 2005. Universal scaling of dissolved oxygen distribution at the sediment-water interface: A power law. Limnol. Oceanogr. 50:1667-1676 [doi:10.4319/lo.2005.50.5.1667].

Jankowski, T., D. M. Livingstone, H. Bührer, R. Forster, and P. Niederhauser. 2006. Consequences of the 2003 European heat wave for lake temperature profiles, thermal stability, and hypolimnetic oxygen depletion: Implications for a warmer world. Limnol. Oceanogr. 51:815-819 [doi:10.4319/lo.2006.51.2.0815].

Jørgensen, B. B. 2001. Life in the diffusive boundary layer, p. 348-373. *In* B. P. Boudreau and B. B. Jørgensen [eds.], The benthic boundary layer: Transport processes and biogeochemistry. Oxford University Press.

———, and N. P. Revsbech. 1985. Diffusive boundary layers and the oxygen uptake of sediments and detritus. Limnol. Oceanogr. 30:111-122 [doi:10.4319/lo.1985.30.1.0111].

———, and D. J. Des Marais. 1990. The diffusive boundary layer of sediments: Oxygen microgradients over a microbial mat. Limnol. Oceanogr. 35:1343-1355 [doi:10.4319/lo.1990.35.6.1343].

———, and B. P. Boudreau. 2001. Diagenesis and sediment-water exchange, p. 211-244. *In* B. P. Boudreau and B. B. Jørgensen [eds.], The benthic boundary layer: Transport processes and biogeochemistry. Oxford University Press.

Krantzberg, G. 1985. The influence of bioturbation on physical, chemical and biological parameters in aquatic environments: A review. Environ. Pollut. Ser. A. 39:99-122 [doi:10.1016/0143-1471(85)90009-1].

Lavery, P. S., C. E. Oldham, and M. Ghisalberti. 2001. The use of Fick's first law for predicting porewater nutrient fluxes under diffusive conditions. Hydrol. Process. 15:2435-2451 [doi:10.1002/hyp.297].

Lewandowski, J., K. Rüter, and M. Hupfer. 2002. Two-dimensional small-scale variability of pore water phosphate in freshwater lakes: Results from a novel dialysis sampler. Environ. Sci. Technol. 36:2039-2047 [doi:10.1021/es0102538].

———, C. Laskov, and M. Hupfer. 2007. The relationship between *Chironomus plumosus* burrows and the spatial distribution of pore-water phosphate, iron and ammonium in lake sediments. Freshwater Biol. 52:331-343 [doi:10.1111/j.1365-2427.2006.01702.x].

Li, Y.-H., and S. Gregory. 1974. Diffusion of ions in sea water and in deep-sea sediments. Geochem. Cosmochim. Acta 38:703-714 [doi:10.1016/0016-7037(74)90145-8].

Lorke, A., L. Umlauf, T. Jonas, and A. Wüest. 2002. Dynamics of turbulence in low-speed oscillating bottom-boundary layers of stratified basins. Environ. Fluid Mech. 2:291-313 [doi:10.1023/A:1020450729821].

———, B. Müller, M. Maerki, and A. Wüest. 2003. Breathing sediments: The control of diffusive transport across the sediment-water interface by periodic boundary-layer turbulence. Limnol. Oceanogr. 48:2077-2085 [doi:10.4319/lo.2003.48.6.2077].

Lorrai, C., D. F. McGinnis, P. Berg, A. Brand, and A. Wüest. 2010. Application of oxygen eddy correlation in aquatic systems. J. Atmos. Oceanic Technol. 27:1533-1546 [doi:10.1175/2010JTECHO723.1].

Mackenthun, A. A., and H. G. Stefan. 1998. Effect of flow velocity on sediment oxygen demand: Experiments. J. Environ. Eng.-ASCE 124:222-230 [doi:10.1061/(ASCE)0733-9372(1998)124:3(222)].

Maerki, M., B. Wehrli, C. Dinkel, and B. Müller. 2004. The influence of tortuosity on molecular diffusion in freshwater sediments of high porosity. Geochem. Cosmochim. Acta 68:1519-1528 [doi:10.1016/j.gca.2003.09.019].

———, B. Müller, and B. Wehrli. 2006. Microscale mineralization pathways in surface sediments: A chemical sensor study in Lake Baikal. Limnol. Oceanogr. 51:1342-1354 [doi:10.4319/lo.2006.51.3.1342].

Müller, B., M. Maerki, C. Dinkel, R. Stierli, and B. Wehrli. 2002. In situ measurements in lake sediments using ion-selective electrodes with a profiling lander system, p. 126-143. *In* M. Taillefert and T. F. Rozan [eds.], Environmental electrochemistry: Analyses of trace element biogeochemistry. ACS symposium series 811, ACS, Washington DC.

Nielsen, L. P., P. B. Christensen, N. P. Revsbech, and J. Sørensen. 1990. Denitrification and oxygen respiration in biofilms studied with a microsensor for nitrous oxide and oxygen. Microb. Ecol. 19:63-72 [doi:10.1007/BF02015054].

Nishihara, G. N., and J. D. Ackerman. 2007. On the determination of mass transfer in a concentration boundary layer. Limnol. Oceanogr. Methods 5:88-96.

———, and J. D. Ackerman. 2009. Diffusive boundary layers do not limit the photosynthesis of the aquatic macrophyte *Vallisneria Americana* at moderate flows and saturating light levels. Limnol. Oceanogr. 54:1874-1882.

O'Connor, B. L., and J. W. Harvey. 2008. Scaling hyporheic exchange and its influence on biogeochemical reactions in aquatic ecosystems. Water Resour. Res. 44: W12423 [doi:10.1029/2008WR007160].

———, and M. Hondzo. 2008. Dissolved oxygen transfer to sediments by sweep and eject motions in aquatic environments. Limnol. Oceanogr. 53:566-578.

———, ———, and J. W. Harvey. 2009. Incorporating both physical and kinetic limitations in quantifying dissolved oxygen flux to aquatic sediments. J. Environ. Eng.-ASCE 135:1304-1314 [doi:10.1061/(ASCE)EE.1943-7870.0000093].

Polerecky, L., N. Volkenborn, and P. Stief. 2006. High temporal resolution oxygen imaging in bioirrigated sediments.

Environ. Sci. Technol. 40:5763-5769 [doi:10.1021/es060494l].

Rabouille, C., L. Denis, K. Dedieu, G. Stora, B. Lansard, and C. Grenz. 2003. Oxygen demand in coastal marine sediments: Comparing in situ microelectrodes and laboratory core incubations. J. Exp. Mar. Biol. Ecol. 285:49-69 [doi:10.1016/S0022-0981(02)00519-1].

Rasmussen, H., and B. B. Jørgensen. 1992. Microelectrode studies of seasonal oxygen uptake in a coastal sediment: Role of molecular diffusion. Mar. Ecol. Prog. Ser. 81:289-303 [doi:10.3354/meps081289].

Reichert, P. 1994. AQUASIM: A tool for simulation and data analysis of aquatic systems. Water Sci. Tech. 30:21-30.

Røy, H., M. Huettel, and B. B. Jørgensen. 2002. The role of small-scale sediment topography for oxygen flux across the diffusive boundary layer. Limnol. Oceanogr. 47:837-847 [doi:10.4319/lo.2002.47.3.0837].

Røy, H., ———, and ———. 2004. Transmission of oxygen concentration fluctuations through the diffusive boundary layer overlying aquatic sediments. Limnol. Oceanogr. 49:686-692 [doi:10.4319/lo.2004.49.3.0686].

Santschi, P., P. Höhener, G. Benoit, and M. Buchholtz-ten Brink. 1990. Chemical processes at the sediment-water interface. Mar. Chem. 30:269-315 [doi:10.1016/0304-4203(90)90076-O].

Urban, N. R., C. Dinkel, and B. Wehrli. 1997. Solute transfer across the sediment surface of a eutrophic lake: I. Porewater profiles from dialysis samplers. Aquat. Sci. 59:1-25 [doi:10.1007/BF02522546].

Zimmerman, J. B., J. R. Mihelcic, and J. Smith. 2008. Global stressors on water quality and quantity. Environ. Sci. Technol. 42:4247-4254 [doi:10.1021/es0871457].

Zhang, H., W. Davison, and C. Ottley. 1999. Remobilisation of major ions in freshly deposited lacustrine sediment at overturn. Aquat. Sci. 61:354-361 [doi:10.1007/s000270050071].

Submitted 18 February 2010
Revised 3 September 2010
Accepted 20 September 2010